Removal of Boron and Phosphorus from Silicon Using CaO-SiO2-Na2O-Al2O3 Flux

Mark Li, Torstein Utigard and Mansoor Barati

Removal of boron and phosphorus from silicon using $CaO\text{-}SiO_2\text{-}Na_2O\text{-}Al_2O_3$ flux

Mark Xiang LI, Torstein UTIGARD, and Mansoor BARATI*

Department of Material Science and Engineering, The University of Toronto,

184 College Street, Toronto, Ont., Canada M5S 3E4

Contact email: mark.li@mail.utoronto.ca

Abstract: A combination of solvent refining and flux treatment was employed to remove boron and phosphorus from crude silicon to acceptable levels for solar applications. Metallurgical grade silicon (MG-Si) was alloyed with pure copper, and the alloy was subjected to refining by liquid $CaO\text{-}SiO_2\text{-}Na_2O\text{-}Al_2O_3$ slags at 1500 °C. The distribution of B and P between the slags and the alloy was examined under a range of slag compositions, varying in $CaO{:}SiO_2$ and $SiO_2{:}Al_2O_3$ ratios and the amount of Na_2O. The results showed that both basicity and oxygen potential have a strong influence on the distributions of B and P. With silica affecting both parameters in these slags, a critical P_{O_2} could be identified that yields the highest impurity pick–up. The addition of Na_2O to the slag system was found to increase the distributions of boron and phosphorus. A thermodynamic evaluation of the system showed that alloying copper with MG-Si leads to substantial increase of boron distribution coefficient. The highest boron and phosphorus distribution coefficients are 47 and 1.1, respectively. Using these optimum slags to reduce boron and phosphorus in MG-Si to solar grade level, a slag mass about 0.3 times and 17 times mass of alloy would be required, respectively.

Key words: Metallurgical silicon, Solar silicon, Slag treatment, Boron, Phosphorus.

1. Introduction

The use of fossil fuels has been associated to the release of greenhouse gases, leading to global warming. As a consequence the need for renewable and clean energy has increased. Among various renewable energy sources such as biomass, wind and hydro power, solar energy is most abundant, noting that Sun's energy received by earth in one minute, if fully harvested, can supply the world's energy demand of an entire year.[1] However, the high manufacturing costs of photovoltaic cells have hampered the widespread use of solar energy even with the government subsidies. Today's US residential solar electricity price ranges from 29 to 64 cents/kWh, which is approximately 3 to 6 times larger than the fossil fuel or nuclear energy based electricity.[2, 3] One of the major cost items of the photovoltaic cells is the cost of high purity silicon, accounting for one third of the finished module cost.[4, 5]

In recent years considerable research has been conducted on refining of metallurgical grade silicon (MG-Si, purity>96%) to solar grade silicon (SoG-Si), with the ultimate goal of reducing the production cost. Metallurgical refining routes have drawn the most attention due to the low operational cost. The reduction of the impurities in silicon to a certain level has to be achieved for a high efficiency solar cell, since the impurities dictate the device performance. Among various elements, Al, As, B, and P are considered most detrimental due to the doping effect they have on Si.

Directional solidification as a well-established process can remove those impurities with low segregation coefficients, but has little effect on boron and phosphorous that possess segregation coefficients substantially above any other impurity.[6, 7]

Vacuum refining, an alternative metallurgical purification method may be used for removing elements with high vapor pressure, such as P and Ca.[8] However, long processing time and the need for extra low vacuum levels make this method unattractive.

Solvent refining is another possible method of removing boron and phosphorous. By alloying silicon with other metals, such as Al, Fe, and Cu which have higher affinity for impurities in liquid phase, the segregation coefficients of boron and phosphorous would be decreased.[9-24] During solidification, pure primary silicon phase in dendrite form precipitates out first, and impurities remain in the eutectic structure. However, the method may not be effective as a one–step purification technique as the data show that the

segregation of impurities between the eutectic and Si is not large enough to achieve SoG–Si specifications. In addition, if the impurities are rejected to the eutectic phase only, the rise in their concentrations prohibits the frequent use of the same alloy for subsequent batches, hence the need for cleaning or sale of the eutectic alloy after several refining cycles.

Oxidizing/slagging treatment is another metallurgical refining technique in which with the use of a proper flux, boron and phosphorous are oxidized to the slag phase according to Reactions (1) and (2).

$$[B] + (3/2)O^{2-} + (3/4)O_2 = (BO_3^{3-}) \qquad (1)$$

$$[P] + (3/2)O^{2-} + (5/4)O_2 = (PO_4^{3-}) \qquad (2)$$

Suzuki *et al.*[25] have determined the equilibrium distribution of boron for a number of slag systems, such as CaO-SiO_2, CaO-CaF_2-SiO_2, CaO-MgO-SiO_2(-CaF_2) and CaO-BaO-SiO_2(-CaF_2), as a function of slag compositions at 1723 to 1873 K under Ar atmosphere. The use of SiO_2 in slag reduces the basicity, but prevents unacceptably high losses of silicon to the slag. Teixeira *et al.*[26] have shown that increasing Na_2O in the flux increased the boron distribution ratio, L_B, and decreased the flux melting temperature. However, it has been discussed that under optimized conditions and highest distribution ratios of 6 and 3 for boron and phosphorous respectively, still a prohibitive amount of slag is required for sufficient refining.[26,27]

A fluxing approach to refine MG-Si, along with alloying with pure copper in the molten state is proposed in the present investigation. This treatment combines solvent refining and slag treatment techniques in one step to achieve high purity Si without contaminating the etutecic alloy excessively. Silicon is alloyed with copper to (a) increase the alloy density for easy phase separation between the molten slag and the alloy, (b) decrease the alloy melting temperature, enabling the use of a more reactive flux at low temperature that is otherwise very corrosive (at high temperature), and (c) allow precipitation of silicon from melt and improve its purity through gettering mechanism. The solvent refining aspect of the study will be discussed in a future publication.

In the present work, the distribution coefficients of B and P in the Si-Cu melt, and the activity coefficients of B_2O_3 in the slag phase were evaluated at 1500℃ and their

relationships with basicity were studied. The values of activity coefficients of B and P in Si-Cu melts were estimated based on Gibbs-Duhem integration. The estimated value of γ_B was compared with the experimental result. Finally, the effects of addition of Na_2O to the slag and alloying Si with pure copper on the distribution coefficients of B and P were also investigated.

2. Experimental

The concentrations of boron and phosphorus in as-received MG-Si were lower than 20 ppmw, which makes the analysis of the purified silicon difficult. Therefore, a 30wt%Si-Cu alloy doped with B and P was used to carry out all the experiments. Boron and phosphorus in the doped alloy were maintained around 3000ppm each. The CaO-Na_2O-Al_2O_3-SiO_2 fluxes with the desired composition were prepared by weighing reagent grade oxides and blending them thoroughly before each experiment. 10 gram of flux was charged into an alumina crucible, and the crucible was heated to 1500℃ in a resistance furnace under Ar atmosphere. When the fluxes were fully molten, 1 gram of solid doped alloy was released into the molten flux. At the end of the experiment, the crucible containing the molten alloy and slag was quenched in a water bath. After drying, the slag and metal phases were separated from crucible and ground to powder for chemical analysis. The time required to achieve equilibrium between slag and alloy was determined by a preliminary set of experiments. Fig.1 presses the results, showing that after approximately 10 minutes the equilibrium has been established. Subsequently, a reaction time of 10 mins was used in the refining experiments at 1500℃. The recent work done by Safarian *et al.*[28] shows that the B equilibrium between slag/melt phases by applying Na_2O-SiO_2 slag was established within 15 mins.

Alloy samples before and after refining were digested in a mixture of nitric and hydrofluoric acids in Teflon beaker at about 45℃ and the B and P in the solutions were analyzed by ICP-AES (Optima ICP 7100DV). Slags were fused with potassium hydroxide in Zirconium crucible at 450℃ and then digested in dilute hydrochloric acid prior to ICP analysis for the trace elements, such as B, P and Fe. The major constituents of the slags were measured by XRF analysis.

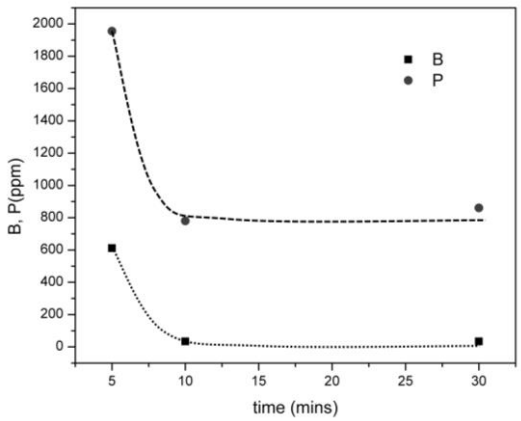

Fig 1. Variation in B and P contents in doped Si-Cu alloys over time for starting composition of 31wt%CaO-20%Na_2O-24%Al_2O_3-25%SiO_2 at 1500℃.

3. Results

As seen in Table 1, the final slag composition determined by XRF was different from its initial composition due to the partial oxidation of silicon and dissolution of alumina crucible in the slag, as well as the Na_2O evaporation. The distribution data are accordingly presented as a function of the final slag composition.

Table 1. Composition of slags before and after equilibrium refining experiments.

	Initial Composition (wt%)				Final composition (wt%)			
Test ID	Na_2O	Al_2O_3	SiO_2	CaO	Na_2O	Al_2O_3	SiO_2	CaO
Test 1-1	20	24	20	36	11.0	26.2	26.9	34.3
Test 1-2	20	24	20	36	11.0	25.2	27.6	34.0
Test 1-3	20	24	20	36	10.8	26.3	27.6	34.6
Test 1-4	20	24	20	36	10.7	27.6	26.9	34.2
Test 1-5	20	24	20	36	10.1	26.3	27.5	34.0
Test 1-6	20	24	28	28	15.7	26.3	31.5	26.0
Test 1-7	20	24	31	25	17.0	24.2	34.8	22.6
Test 1-8	20	24	36	20	19.7	24.4	37.3	18.2
Test 1-9	20	24	41	15	21.1	23.8	41.2	13.5
Test 1-10	20	24	46	10	20.8	23.0	46.5	9.0
Test 2-1	20	8	36	36	14.1	18.0	36.9	29.8
Test 2-2	20	11	33	36	13.5	18.5	35.7	31.3
Test 2-3	20	14	30	36	12.6	19.6	34.3	32.5
Test 2-4	20	17	27	36	13.3	20.6	32.1	33.5
Test 2-5	20	20	24	36	11.8	22.4	30.4	33.9
Test 2-6	20	26	18	36	10.1	28.5	25.5	35.2
Test 3-1	0	21	34	45	0.2	20.1	36.4	42.4
Test 3-2	5	20	32	43	4.6	21.6	34.0	38.7
Test 3-3	10	19	30	41	6.8	31.6	27.6	33.5
Test 3-4	15	18	29	38	7.1	26.3	27.6	30.3
Test 3-5	15	18	29	38	7.3	23.9	29.1	32.2
Test 3-6	20	17	27	36	13.3	20.6	32.1	33.5
Test 3-7	30	15	24	32	17.7	20.8	31.7	28.9

The B and P contents in the slag and silicon and the distribution coefficients of B and P are summarized in Table 2. The distribution coefficient is the ratio of the concentration (in ppmw) of impurity M in the slag to that in the metal after refining. The ratio can be expressed as

$$L_M = \frac{(M)}{[M]} \quad (3)$$

Table 2. B and P distributions between silicon and slag phases of the $CaO\text{-}SiO_2\text{-}Al_2O_3\text{-}Na_2O$ system for various slag compositions at 1500℃

Test ID	$(B)_{slag}$ ppmw	$[B]_{metal}$ ppmw	$(P)_{slag}$ ppmw	$[P]_{metal}$ ppmw	L_B	L_P
Test 1-1	293	10	435	637	30.9	0.68
Test 1-2	329	14	339	623	23.5	0.54
Test 1-3	343	10	247	452	34.6	0.55
Test 1-4	347	17	217	645	20.2	0.34
Test 1-5	383	11	238	579	36.3	0.41
Test 1-6	357	23	254	753	15.6	0.34
Test 1-7	274	16	245	953	16.7	0.26
Test 1-8	282	22	132	1368	12.7	0.1
Test 1-9	348	37	76	2198	9.4	0.03
Test 1-10	241	374	63	2565	0.7	0.02
Test 2-1	265	20	190	544	13.0	0.35
Test 2-2	255	6	209	458	40.2	0.46
Test 2-3	297	6	274	489	46.8	0.56
Test 2-4	275	7	181	434	42.3	0.42
Test 2-5	241	10	218	735	25.3	0.30
Test 2-6	345	19	234	667	18.7	0.35
Test 3-1	348	15	135	1785	22.7	0.08
Test 3-2	381	14	255	1114	26.9	0.23
Test 3-3	281	10	363	380	28.3	0.96
Test 3-4	321	7	301	350	44.6	0.86
Test 3-5	326	8	305	278	41.8	1.10
Test 3-6	275	7	181	434	42.3	0.42
Test 3-7	248	11	212	1313	21.8	0.16

3.1 Slags with Varying CaO: SiO_2

The influence of slag basicity on removal of impurities from Si-Cu alloy was investigated by varying $CaO:SiO_2$ ratios of the $CaO\text{-}Na_2O\text{-}Al_2O_3\text{-}SiO_2$ slag, while maintaining the initial concentrations of Na_2O and Al_2O_3 at 20 and 24wt%, respectively. Treatment of Cu–Si alloy with a 36wt%CaO-20wt%SiO_2-20wt%Na_2O-Al_2O_3 flux was repeated five times under similar experimental conditions. The average value of the distributions is shown at CaO/SiO_2 ratio =1.25, with one standard deviation of uncertainty. It may suggest that good repeatability has been achieved in current experiment, noting the inherent difficulties and uncertainties in high temperature experiments.

For both boron and phosphorus, the strong dependence of L_M on basicity is clear. The

distribution coefficients increase linearly with basicity over the entire range studied. The values of L_B are much greater than unity for all experiments, and the maximum reached is approximately 29, indicating that boron reports preferentially to the slag phase. In comparison, the values obtained by other researchers are significantly lower (Figure XYZ), also some appear to go through a maximum when increasing the basicity. The reason for the differences will be discussed in Section 4. Although L_P increases with basicity, the actual values of L_P are all less than unity, indicating that phosphorus favors the alloy phase.

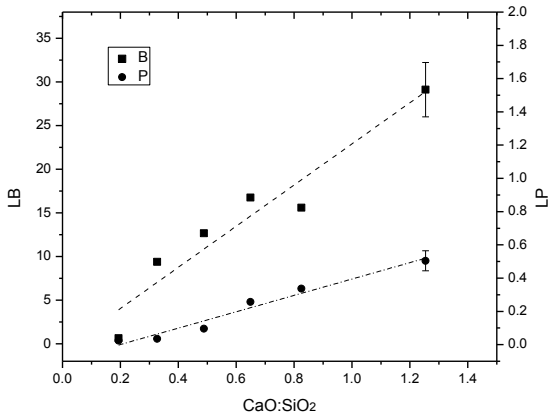

Fig 2. Distribution coefficients of impurities between slag and Si-Cu alloy as a function of the final basicity of the slag equilibrated at 1500℃.

HERE XYZ

3.2 Slags with Varying SiO_2:Al_2O_3

Impurity removal from Si-Cu alloy was investigated with different oxygen potentials of the slag by varying SiO_2:Al_2O_3 ratios of the CaO-Na_2O-Al_2O_3-SiO_2 slag. Values of L_M are illustrated in Fig 3 against the final SiO_2:Al_2O_3 ratios. In these experiments, the initial CaO and Na_2O were fixed at 36 and 20wt%, respectively. Values for boron and phosphorus follow a similar trend as they increase with increasing ratio of SiO_2:Al_2O_3 until reaching a maximum at SiO_2:Al_2O_3 around 1.7. These results suggest that the

distribution coefficients of boron and phosphorus are strongly affected by both the oxygen potential and the basicity of the slag in the studied range of SiO_2:Al_2O_3 ratio. With increasing SiO_2:Al_2O_3, on one hand the oxygen potential is increased, and on the other hand, the slag becomes less basic as SiO_2 is more acidic in nature than Al_2O_3. This is evident by the fact that the optical basicity (Λ) of SiO_2 (0.48) is lower than that of Al_2O_3 (0.61).[29] The values of L_B are still much greater than unity for all experiments, and the maximum reached is 47, indicating again the preference of boron for the slag phase. All L_P values are less than unity, indicating a preference to remain in the alloy phase.

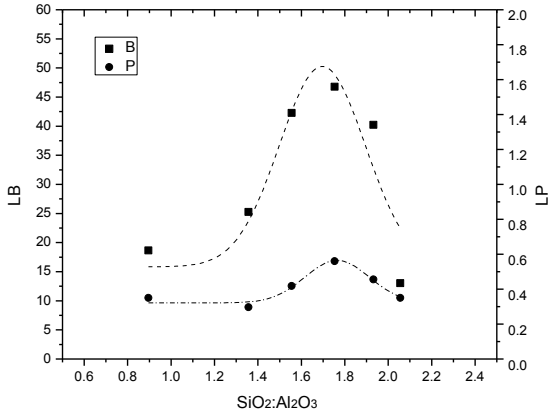

Fig 3. Distribution coefficients of impurities between slag and Si-Cu alloy as a function of SiO_2:Al_2O_3 ratios of slag equilibrated at 1500℃.

3.3 Slags with Varying Na_2O content

The influence of Na_2O addition to the slag on removal of impurities from Si-Cu alloy was investigated by varying the amount of Na_2O added into the CaO-Na_2O-Al_2O_3-SiO_2 slag. Values of L_M are illustrated in Fig 4 against the starting weight percentage of Na_2O added into the slag. The mass ratio of CaO:Al_2O_3:SiO_2 in these slags remained constant at 45:21.25:33.75, and the Na_2O content was varied 0, 5, 10, 15, 20 and 30wt%. The best fitting curves show that the distribution coefficients go through a maximum at 15-20wt% Na_2O and 10-15wt% Na_2O for B and P, respectively. Further addition of Na_2O to the slag

decreases the distribution coefficients. For phosphorus, the effect of Na_2O on L_p is similar at 30wt% and at 5wt%. By comparing Na_2O free slag (0wt% Na_2O in Fig 4), the distributions of boron and phosphorus can be increased by a factor of up to 2 and 7, respectively. The trend and extent of B distribution changing with the increasing Na_2O are similar to that reported by Teixeira *et al* until the Na_2O addition is up to 10wt%.[26] The decline of L_B after reaching the local maximum with further Na_2O addition was observed by Hu *et al* and Tanahashi *et al*.[30,31]

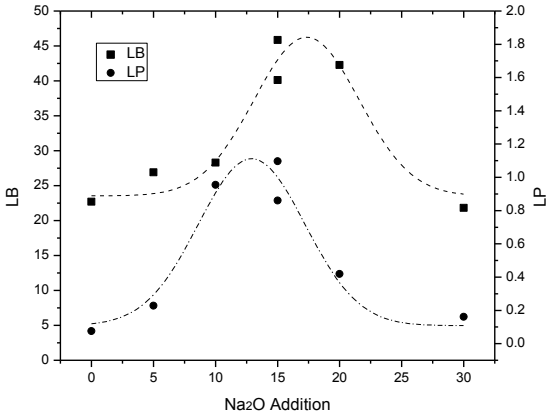

Fig 4. Effect of addition of Na_2O on the distribution coefficients of impurities at 1500℃

4. Discussion

4.1 Dependence of distributions on basicity and oxygen potential

According to Reactions 1 and 2, boron and phosphorus enter a basic slag phase as oxides with silica acting as the oxidizing agent. In each case, oxygen ions are provided by the basic components such as CaO and Na_2O and the oxygen partial pressure (P_{O_2}) is established by Si-SiO_2 equilibrium.

$$(CaO) = Ca^{2+} + O^{2-} \quad (4)$$

$$(Na_2O) = 2Na^{+} + O^{2-} \quad (5)$$

$$(SiO_2) = [Si] + O_2 \quad (6)$$

The equilibrium constants for Reaction (1) and (2) are shown in Equations (7) and (8), where f_M and $f_{MO_n^{3-}}$ are the activity coefficients of species M and MO_n^{3-} in liquid alloy and slag with respect to a 1 mass pct standard state. Constants C_1 and C_2 are conversion factors of mass% of BO_3^{3-} and PO_4^{3-} to mass% of boron and phosphorus in the slag phase, and constants C_3 and C_4 are factors for converting the standard state of dissolved M from 1 mass pct M to pure liquid M.

$$K_1 = \frac{a_{BO_3^{3-}}}{a_B \cdot a_{O_2}^{3/4} \cdot a_{O^{2-}}^{3/2}} = \frac{C_1(B) \cdot f_{BO_3^{3-}}}{[B] \cdot f_B \cdot P_{O_2}^{3/4} \cdot a_{O^{2-}}^{3/2}} = \frac{C_1(B) \cdot f_{BO_3^{3-}}}{C_3 \cdot [B] \cdot \gamma_B \cdot P_{O_2}^{3/4} \cdot a_{O^{2-}}^{3/2}} \quad (7)$$

$$K_2 = \frac{a_{PO_4^{3-}}}{a_P \cdot a_{O_2}^{5/4} \cdot a_{O^{2-}}^{3/2}} = \frac{C_2 \cdot (P) \cdot f_{PO_4^{3-}}}{[P] \cdot f_P \cdot P_{O_2}^{5/4} \cdot a_{O^{2-}}^{3/2}} = \frac{C_2 \cdot (P) \cdot f_{PO_4^{3-}}}{C_4 \cdot [P] \cdot \gamma_P \cdot P_{O_2}^{5/4} \cdot a_{O^{2-}}^{3/2}} \quad (8)$$

Equations (7) and (8) can be rearranged to yield the distribution coefficients as Equations (9) and (10), where constants C_5 and C_6 are ratios of C_1 to C_3 and C_2 to C_4, respectively, and K_6 is the equilibrium constant for Reaction (5).

$$L_B = \frac{(B)}{[B]} = K_1 C_5 \frac{\gamma_B \cdot P_{O_2}^{3/4} \cdot a_{O^{2-}}^{3/2}}{f_{BO_3^{3-}}} = K_1 C_5 \frac{\gamma_B \cdot a_{O^{2-}}^{3/2}}{f_{BO_3^{3-}}} \cdot \left(\frac{K_6 \cdot a_{SiO_2}}{a_{Si}}\right)^{\frac{3}{4}} \quad (9)$$

$$L_P = \frac{(P)}{[P]} = K_2 C_6 \frac{\gamma_P \cdot P_{O_2}^{5/4} \cdot a_{O^{2-}}^{3/2}}{f_{PO_4^{3-}}} = K_2 C_6 \frac{\gamma_P \cdot a_{O^{2-}}^{3/2}}{f_{PO_4^{3-}}} \cdot \left(\frac{K_6 \cdot a_{SiO_2}}{a_{Si}}\right)^{\frac{5}{4}} \quad (10)$$

In order to isolate the effect of basicity, the distribution coefficients were normalized with respect to P_{O_2} at each slag composition. The normalized distribution (D_M) of impurity M, was calculated as follows:

$$D_M = \frac{L_M}{(P_{O_2})^n} = \frac{(M)}{[M]} \left(\frac{a_{Si}}{K_6 \cdot a_{SiO_2}}\right)^n = K_{1,2} C_{5,6} \frac{\gamma_M \cdot a_{O^{2-}}^{3/2}}{f_{MO_n^{3-}}} \quad (11)$$

The contents of impurities in slag and alloy phases, silicon in the refined alloy, and silica in the slag were measured after refining. The activity of silica was determined by thermodynamic calculation with measured concentrations using FactSage™.[32,33] The value of the activity of silicon was taken from the work of Miki *et al.*[34] K_6, the equilibrium constant between SiO_2 and Si was obtained from FactSage™, and P_{O_2} was calculated from the equilibrium between SiO_2 and Si. The power *n* in Eq. (11) is 3/4 for

boron and 5/4 for phosphorus. As optical basicity can be used as a measure of $a_{O^{2-}}$, Fig5 plots the normalized distribution data for boron and phosphorus against the corrected optical basicity (Λ_{corr}) of slag. The corrected optical basicity and oxygen partial pressure of different slag systems are listed in Table 3. As predicted, the normalize distributions of B and P increase with an increasing Λ_{corr}.

As Fig 5 shows, the normalized distributions of B and P for the three sets of experiments lie on the same line, where for each impurity $\log D_M$ increase linearly with the corrected optical basicity. It appears that in the composition range covered in the present study, the ratios of activity coefficients of boron and phosphorus (γ_B, γ_P) to their oxides ($f_{BO_3^{3-}}, f_{PO_4^{3-}}$) do not change considerably, as the relationships remain linear regardless of the change in alloy and slag composition.

The relationship between D_M and Λ_{corr} can be derived from the trend lines in Fig. 5

$$\log D_B = 25.7\Lambda_{corr} - 0.82 \quad (12)$$

$$\log D_P = 31.6\Lambda_{corr} + 2.99 \quad (13)$$

Table 3. Thermodynamic data of the $CaO\text{-}SiO_2\text{-}Al_2O_3\text{-}Na_2O$ system at 1500℃.

Test ID	Λ_{corr}	P_{O_2}(atm)	γ_B	γ_P	a_B	a_P	a_{Si}	a_{SiO_2}	$C_{BO_3^{3-}}$	$C_{PO_4^{3-}}$
Test 1-1	0.650	8.05×10^{-20}	1.18	0.023	5.70×10^{-5}	2.63×10^{-5}	0.07	1.95×10^{-3}	5.86×10^{17}	3.74×10^{27}
Test 1-2	0.650	8.2×10^{-20}	1.17	0.025	8.28×10^{-5}	2.69×10^{-5}	0.08	2.28×10^{-3}	4.46×10^{17}	2.78×10^{27}
Test 1-3	0.648	1.14×10^{-19}	1.19	0.021	6.10×10^{-5}	1.73×10^{-5}	0.06	2.34×10^{-3}	4.93×10^{17}	2.10×10^{27}
Test 1-4	0.646	1.17×10^{-19}	1.20	0.021	1.06×10^{-4}	2.40×10^{-5}	0.06	2.27×10^{-3}	2.81×10^{17}	1.28×10^{27}
Test 1-5	0.644	1.18×10^{-19}	1.18	0.024	6.32×10^{-5}	2.41×10^{-5}	0.08	3.05×10^{-3}	5.18×10^{17}	1.38×10^{27}
Test 1-6	0.628	9.67×10^{-20}	1.09	0.040	1.18×10^{-4}	4.97×10^{-5}	0.17	5.46×10^{-3}	3.00×10^{17}	9.16×10^{26}
Test 1-7	0.620	1.90×10^{-19}	1.08	0.042	8.34×10^{-5}	6.50×10^{-5}	0.18	1.12×10^{-2}	1.96×10^{17}	2.90×10^{26}
Test 1-8	0.612	2.24×10^{-19}	1.04	0.051	1.06×10^{-4}	1.11×10^{-4}	0.23	1.66×10^{-2}	1.41×10^{17}	7.43×10^{25}
Test 1-9	0.598	4.84×10^{-19}	1.05	0.050	1.78×10^{-4}	1.75×10^{-4}	0.22	3.48×10^{-2}	5.79×10^{17}	1.04×10^{25}
Test 1-10	0.577	7.80×10^{-19}	0.99	0.066	1.62×10^{-3}	2.58×10^{-4}	0.29	7.42×10^{-2}	3.08×10^{15}	3.21×10^{24}
Test 2-1	0.641	2.59×10^{-19}	1.10	0.037	2.17×10^{-4}	6.72×10^{-5}	0.15	1.28×10^{-2}	5.79×10^{16}	1.49×10^{26}
Test 2-2	0.645	1.67×10^{-19}	1.08	0.041	3.25×10^{-5}	3.08×10^{-5}	0.17	9.55×10^{-3}	5.19×10^{17}	6.15×10^{26}
Test 2-3	0.645	1.49×10^{-19}	1.10	0.038	3.32×10^{-5}	3.09×10^{-5}	0.16	7.78×10^{-3}	6.41×10^{17}	9.25×10^{26}
Test 2-4	0.653	6.40×10^{-20}	1.07	0.044	3.27×10^{-5}	3.08×10^{-5}	0.17	3.60×10^{-3}	1.14×10^{18}	1.77×10^{27}
Test 2-5	0.650	5.11×10^{-20}	1.06	0.047	4.68×10^{-5}	5.52×10^{-5}	0.21	3.44×10^{-3}	8.24×10^{17}	1.57×10^{27}
Test 2-6	0.649	2.87×10^{-20}	1.07	0.044	9.24×10^{-5}	4.81×10^{-5}	0.19	1.82×10^{-3}	9.22×10^{17}	3.98×10^{27}

Commented [M1]: Check the calculations. Also, show Log values

test 3-1	0.635	5.30×10^{-19}	1.01	0.060	6.92×10^{-5}	1.66×10^{-4}	0.26	4.61×10^{-2}	1.39×10^{17}	1.74×10^{25}
test 3-2	0.638	2.70×10^{-19}	1.06	0.047	6.92×10^{-5}	8.44×10^{-5}	0.21	1.86×10^{-2}	2.53×10^{17}	1.50×10^{26}
test 3-3	0.624	1.09×10^{-19}	1.05	0.048	4.82×10^{-5}	2.95×10^{-5}	0.21	7.65×10^{-3}	5.31×10^{17}	1.34×10^{27}
test 3-4	0.625	1.71×10^{-19}	1.08	0.041	3.58×10^{-5}	2.36×10^{-5}	0.17	9.66×10^{-3}	5.82×10^{17}	1.13×10^{27}
test 3-5	0.633	2.97×10^{-19}	1.15	0.027	4.61×10^{-5}	1.31×10^{-5}	0.10	9.29×10^{-3}	2.98×10^{17}	1.03×10^{27}
test 3-6	0.653	6.40×10^{-20}	1.07	0.044	3.27×10^{-5}	3.08×10^{-5}	0.17	3.60×10^{-3}	1.14×10^{18}	1.77×10^{27}
test 3-7	0.656	2.89×10^{-20}	1.04	0.051	5.43×10^{-5}	1.06×10^{-4}	0.23	2.15×10^{-3}	1.12×10^{18}	1.62×10^{27}

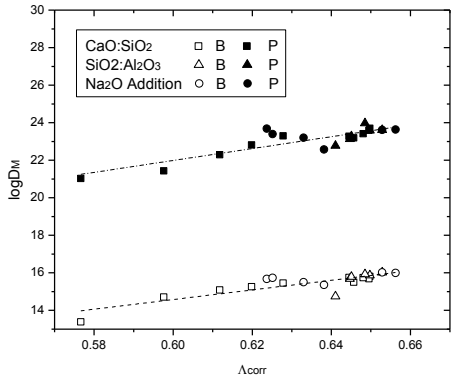

Fig 5. Normalized distribution coefficients of B and P in different slag systems as a function of the corrected optical basicity at 1500℃

Even though D_M can isolate the basicity effect from oxygen potential, it cannot exclude the activity coefficient of M in metal phase. Therefore, borate and phosphate capacitieswere calculated, as a parameter that is only dependent on slag composition and temperature. The oxidation of B and P by slag were shown in Reactions (1) and (2). Based on these two reactions, the borate capacity and Phosphate capacity of the slag are obtained by Equations (14) and (15), respectively.

$$C_{BO_3^{3-}} = \frac{(mass\%BO_3^{3-})}{a_B P_{O_2}^{3/4}} = \frac{K_1 a_{O^{2-}}^{3/2}}{f_{BO_3^{3-}}} \qquad (14)$$

$$C_{PO_4^{3-}} = \frac{(mass\%PO_4^{3-})}{a_P P_{O_2}^{5/4}} = \frac{K_2 a_{O^{2-}}^{3/2}}{f_{PO_4^{3-}}} \qquad (15)$$

where K_1 and K_2 are equilibrium constants of Reactions (1) and (2), respectively. The activities of B and P in liquid alloy were calculated from the activity coefficients of B and

P, which were evaluated from literature data by Gibbs-Duhem integration as expressed in Equation (16). The activity coefficients of B and P in molten silicon/copper and the excess Gibbs energy for mixing in the Si-Cu melt have been measured previously.[34-38] The value of the activity coefficient of P in molten copper at 1500℃ was extrapolated from the value at 1300℃ with the assumption of regular solution. The activity coefficients of B and P at 1500℃ in Cu and Si are shown in Table 4. The data needed to calculate the capacities are listed in Table 3. As expected plots in Figure 6 show that the borate capacity and phosphate capacity increase with the basicity of the slag. The linear relation of capacity against slag basicity is expressed as Equations (17) and (18) for B and P, respectively.

$$RTln\gamma^{\circ}_{i(l)in\ Si-Cu\ alloy} = X_{Si\ in\ Si-Cu\ alloy}RTln\gamma^{\circ}_{i(l)in\ molten\ Si} + X_{Cu\ in\ Si-Cu\ alloy}RTln\gamma^{\circ}_{i(l)in\ molten\ Cu} - \Delta G^{ex}_{Si-Cu\ alloy} \quad (16)$$

Table 4. Activity coefficients of B and P in the Cu and Si melts at 1500℃.

	γ°_B	γ°_P
Si	0.38	0.55
Cu	1.44	0.007

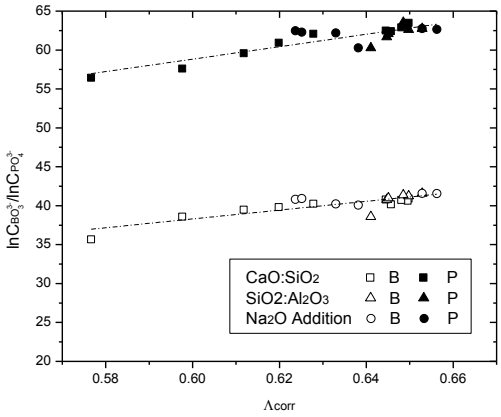

Fig 6 Relationship between the borate and phosphate capacities and the corrected optical basicity at 1500℃

$$lnC_{BO_3^{3-}} = 56.6\Lambda_{\text{corr}} + 4.37 \qquad (17)$$

$lnC_{PO_4^{3-}} = 79.9\Lambda_{\text{corr}} + 10.9$ (18)As mentioned earlier, due to their small concentrations in Si-Cu and slag phases, it may be assumed that the activity coefficients of boron, phosphorus (γ_B, γ_P) and their oxides ($f_{BO_3^{3-}}, f_{PO_4^{3-}}$) do not change considerably over the concentration ranges studied here. As shown in Equations (9) and (10), the distributions of boron and phosphorus are dependent on oxygen potential and basicity of the slag. However, the two parameters compete with each other as both are influenced by a_{SiO_2} and increasing one leads to a decrease in the other. A critical oxygen potential was introduced in the current work to determine where the balance of the two parameters yields the highest distribution ratio. In the system with varying SiO_2:Al_2O_3, the P_{O_2} was low when the ratio was small, so the initial observed increase in L_B and L_P with SiO_2:Al_2O_3 is because of increasing P_{O_2}. However, once the P_{O_2} is beyond the $P_{O_2,critical}$, the effect of the slag basicity overcomes the effect of oxygen potential, leading to a drop in distributions. Distribution coefficients for boron and phosphorus in the system with varying Na_2O follow a similar trend. However, Na_2O addition increased distribution coefficients as Na_2O has a higher optical basicity (Λ=1.15) than all other slag constituents.[29] At the expense of having a highly basic slag, the P_{O_2} in turn is reduced due to stronger effect on lowering a_{SiO_2}. Results in the system with varying CaO:SiO_2 showed that even at the highest ratio 1.3, the smallest value of P_{O_2} was still presumably above the $P_{O_2,critical}$, as the distributions keep increasing with basicity. By comparing the changes of the distributions of B and P with all values of P_{O_2} in Table 3, it was found that $P_{O_2,critical}$ is around $1.5 \times 10^{-19} atm$ and $1.7 \times 10^{-19} atm$ for B and P, respectively.

Considering the effect of basicity, phosphorus should be easier to be removed to a basic slag, as it has a more acidic oxide (Λ =0.4) than boron (Λ =0.42).[29] However, the effect of oxygen potential should be stronger on boron, as its oxide is more stable than phosphorus. The results show that the combined effect of all these factors gives rise to more favorable removal of boron under the examined experimental conditions.

4.2 The effect of alloying on distribution of boron

The distribution coefficient of boron in the present work (0.7–47, Figure ABC) is

considerably higher than those reported by other researchers (0.08–5.5 , Fig. XYZ). Although small variations could be attributed to the different slag composition, the reason for such a significant difference is believed to be the effect of alloying. In the previous studies, slag has been used to treat MG-Si, while in the present study, Si-Cu alloy was subjected to slag treatment.

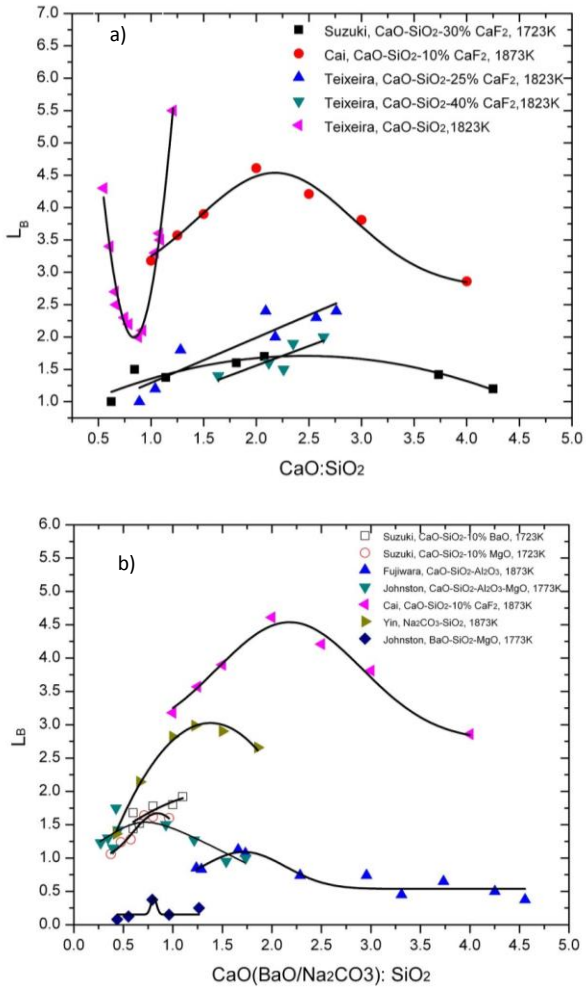

Fig 7 Boron distribution versus a function of slag composition expressed in a) $CaO\text{-}SiO_2$ binary and $CaO\text{-}SiO_2\text{-}CaF_2$ ternary system; b) other slag systems.[39]

Assuming similar slag chemistry, the ratio of the distributions of boron in current work to that reported by Teixeira *et al* and Johnston *et al* is expressed by Equation (19).

$$R = \frac{L_{B,Si-Cu}}{L_{B,MG-Si}} = \left(\frac{\gamma_{B,Si-Cu}}{\gamma_{B,MG-Si}}\right) \cdot \left(\frac{P_{O_2,Si-Cu}}{P_{O_2,MG-Si}}\right)^{3/4} = \left(\frac{\gamma_{B,Si-Cu}}{\gamma_{B,MG-Si}}\right) \cdot \left(\frac{a_{Si,MG-Si}}{a_{Si,Si-Cu}}\right)^{3/4} \quad (19)$$

For a liquid 20wt%Si-Cu alloy, the activity of silicon (a_{Si}) in the liquid alloy is 0.19 compared to $a_{Si} \cong 1$ in liquid MG-Si.[40] As seen in Table 3, the calculated activity coefficients of B in Si-Cu melts are in the range of 1-1.2, which is much larger than the value in silicon melt, 0.38. Considering the combined effects of variations in $\gamma_B$and a_{Si}, up to 10 times increase in the boron distribution is estimated based on Eq. (19). This is consistent with the observed differences in the results of this study and previous works.

Similarly, the ratio of the distribution of phosphorus between the current study and that reported by Johnston and Barati[27] can also be evaluated. However, due to the small value of the activity coefficient of P in Cu melt as seen in Table3, the distribution of P even slightly decreases. Therefore, as expected the values of the distribution coefficient of P in the current work are close to the ones reported by others.[27]

4.3 Impurity removal efficiency

Removal efficiency (R) of impurity M can be expressed as a function of L_M shown as Equation (17), where m_{Si} and m_{slag} are the mass of silicon and slag, respectively.

$$R = \frac{L_M}{L_M + \frac{m_{Si}}{m_{slag}}} \quad (17)$$

In the present work, the highest distribution coefficients were 47 and 1.1 for boron and phosphorus, respectively. To reduce boron and phosphorus from MG-Si with typical initial concentrations of 15 and 20 ppmw to the final level 1 ppmw, the required removal efficiencies are 93% for boron and 95% for phosphorus. To achieve this reduction with the slags that yielded the highest L_M, the slag mass required is roughly 0.3 and 17 times that of metal for B and P removal, respectively. It thus appears that boron removal may be achieved with a reasonable slag mass while meeting the desired phosphorus level is

impractical in industrial scale due to high processing cost and technical challenges associated with large slag volume. These removal efficiencies are however for the slag treatment only. It is expected that the silicon dendrites recovered from the alloy will have higher purity than the Cu-Si melt. This will affect the actual slag mass required.

5. Conclusions

The distributions of boron and phosphorus between CaO-SiO_2-Na_2O-Al_2O_3 slags and Si-Cu alloy were examined at 1500℃ by varying the CaO:SiO_2 and SiO_2:Al_2O_3 ratios and the amount of Na_2O. It was found that:

(1) The distribution coefficient is dependent on both basicity and oxygen potential, which are in part controlled by SiO_2 content of the slag. As a result, a critical oxygen partial pressure ($P_{O_{2,critical}}$) could be defined so that it yields the highest distribution ratios. It is suggested that a strongly basic slag with its P_{O_2} at the critical value would be most efficient for boron and phosphorus pick up.

(2) The highest distribution coefficients of boron and phosphorus were 47 and 1.1, respectively. It therefore appears that removal of only B to desired level is practical using a reasonable amount of slag.

(3) The distribution coefficients of B and P are improved by the addition of Na_2O and go through a maximum at 15-20wt%Na_2O and 10-15wt%Na_2O for B and P respectively, after which they begin to drop.

(4) The primary reason for increased B distribution observed in the present study is believed to be the effect of Cu on the activity coefficient of B and activity of Si.

(5) The borate capacity and phosphate capacity of the CaO-SiO_2-Na_2O-Al_2O_3 slag at 1500℃ can be represented as

$$lnC_{BO_3^{3-}} = 56.6\Lambda_{\text{corr}} + 4.37$$

$lnC_{PO_4^{3-}} = 79.9\Lambda_{\text{corr}} + 10.9$**Acknowledgement**

The present study was partially supported by NSERC.

References

1. *Solar Energy*. [cited 2013 July 3rd]; Available from: http://www.altenergy.org/renewables/solar.html
2. Electric Power Monthly with Data for Februrary 2013, U.S Energy Information Administration, Washingtion, 2013.
3. *Solar electricity Prices*. 2012 March [cited 2013 July 3rd]; Available from: http://www.solarbuzz.com/facts-and-figures/retail-price-environment/solar-electricity-prices.
4. *Solar PV Cell Weekly Spot Price-PVinsights*. June 30, 2013 [cited 2013 July 3rd]; Available from: http://pvinsights.com/index.php.
5. *PV Cells & Modules*. [cited 2013 July 3rd]; Available from: http://www.greenrhinoenergy.com/solar/technologies/pv_modules.php.
6. R. H. Hopkins: *Proc. JPL Proceedings of the Flat-Plate Solar Array Project Workshop*, NASA, California, 1985, pp.215-233.
7. A. Schei: *Proc. Inter. Seminar on Refining and Alloying of Liquid Aluminum and Ferro-Alloys,* Trondheim, Norway, 1985, pp.72-89.
8. J. C. S. Pires, J. Otubo, A. F. B. Braga, and P. R. Mei: *J. of Mater. Processing Tech.*, 2005, vol. 169 (1), pp. 16-20.
9. T. Yoshikawa and K. Morita: *J. of Cryst. Growth*, 2009, vol. 311 (3), pp.776-779.
10. S. Esfahani and M. Barati*, Metals Mater. Int*.2011,vol 17, pp 823-829
11. S. Esfahani and M. Barati, *Metals Mater. Int*. 2011, vol 17, pp 1009-1015
12. A.M. Mitrasinovic´ and T.A. Utigard, *Silicon*,2009, vol 1, pp.239-248
13. T. Miki, K. Morita, and N. Sano, *Metall. Mater. Trans. B*„1996, vol 27,pp.937-941
14 T. Miki, K. Morita, and N. Sano, *Metall. Mater. Trans. B,* 1997, vol 28, pp.861-867
15 T. Miki, K. Morita, and N. Sano, *Metall. Mater. Trans. B*, 1998, vol 29,pp.1043-1049
16. K. Morita and T. Miki, *Intermetallics*, 2003, vol 11, pp.1111-1117.
17. T. Yoshikawa and K. Morita, *Sci. Technol. Adv. Mater.*, 2003, vol 4, pp.531-537
18. T. Yoshikawa and K. Morita, *J. Electrochem. Soc.*, 2003, vol 150, G465-468.
19. T. Yoshikawa, K. Arimura, and K. Morita, *Metall. Mater.Trans. B*, 2005, vol 36, pp. 837-842
20. T. Yoshikawa and K. Morita, *Metall. Mater. Trans. B*, 2005, vol 36, pp.731-736.
21. T. Yoshikawa and K. Morita, *J. Phys. Chem. Solids*, 2005, vol 66, pp.261-265.
22. T. Yoshikawa, K. Morita, in EPD Congress (TMS, Warrendale,PA, 2005), pp.549–558.
23. T. Yoshikawa, K. Morita, S. Kawanishi, and T. Tanaka, *J. Alloys Compd.*, 2010, vol 490, pp.31-41.
24. K. Morita and T. Yoshikawa, *Trans. Nonferrous Metals Soc.China*, 2011, vol 21, pp. 685-690.
25. K. Suzuki: *Nippon Kinzoku Gakkaishi*, 1990, vol. 54 (2), pp. 161-167.
26. L. A. V. Teixeira and K. Morita: *ISIJ int*., 2009, vol. 49 (6), pp. 783-787.
27. M. D. Johnston and M. Barati: *J. of Non-Cryst. Solids*, 2011, vol. 357 (3), pp. 970-975.
28. J. Safarian, G. Tranell, and M. Tangstad, *Metall. Mater. Trans. B*, 2013, vol 44, pp. 571-583.

29. V. D. Eisenhuttenleute: *Slag Atlas*, 2nd ed , Verlag Stahleisen GmbH, Düsseldorf, Germany, 1995.
30. Y. Hu, D. Lu, T, Lin, Y. Liu, B. Wang, C. Guo, Y. Sun, H. Chen, and Q. Li, *Adv. Mater. Res.,* 2011, vol 156-157, pp. 882-885.
31. M. Tanahashi, Y. Shinpo, T. Fujisawa, and C. Yamauchi, *J. Min. Mater. Process. Inst. Jpn.* 2002, vol 118, pp. 497-505.
32. C. W. Bale, P. Chartrand, S. A. Degterov, G. Eriksson, K. Hack, R. Ben Mahfoud, J. Melançon, A.D. Pelton, and S. Petersen: *Calphad*, 2002, vol. 26 (2), pp.189-228.
33. C. W. Bale, E. Bélisle, P. Chartrand, S. A. Decterov, G. Eriksson, K. Hack, I. H. Jung, Y. B. Kang, J. Melançon, A. D. Pelton, C. Robelin, and S. Petersen: *Calphad*, 2009, vol. 33 (2), pp. 295-311.

.
34. D. Ludecke, *Calphad*, 1987, vol. 11, pp135-142.
35. K. T. Jacob, S. Priya, and Y. Waseda: *Metall. and Mater. Trans. A*, 2000, vol. 31(10), pp 2674-2678.
36. A. I. Zaitsev, A. D. Litvina, and N. E. Shelkova: *High Temp*+., 2001, vol. 39(2), pp 227-232.
37. R. Noguchi, K. Suzuki, F. Tsukihashi, and N. Sano: *Metall. and Mater. Trans. B*, 1994, vol. 25(6), pp. 903-907.
38. M. Iwase, E. Ichise, and N. Yamada: *Steel Res.*, 1985, vol. 56, pp. 319-326.
39. M. Johnston, L. Khajavi, M. Li, S. Sokhanvaran, and M. Barati, *JOM*, 2012, vol. 64, pp. 935-945.
40. K. Sano, K. Okajima, and N. Okuda: *Mem. Sch. Eng.*, 1956, vol. 8, pp. 127-130.